

# Large Magnetic Moments of Arsenic-Doped Mn Clusters and their Relevance to Mn-Doped III-V Semiconductor Ferromagnetism

Mukul Kabir,<sup>1,\*</sup> D. G. Kanhere,<sup>2</sup> and Abhijit Mookerjee<sup>1</sup>

<sup>1</sup>*S.N. Bose National Centre for Basic Sciences, JD Block, Sector III, Salt Lake, Kolkata - 700 098, India*

<sup>2</sup>*Department of Physics and Centre for Modelling and Simulation, University of Pune, Pune - 411 007, India*

(Dated: November 6, 2018)

We report electronic and magnetic structure of arsenic-doped manganese clusters from density-functional theory using generalized gradient approximation for the exchange-correlation energy. We find that arsenic stabilizes manganese clusters, though the ferromagnetic coupling between Mn atoms are found only in Mn<sub>2</sub>As and Mn<sub>4</sub>As clusters with magnetic moments  $9 \mu_B$  and  $17 \mu_B$ , respectively. For all other sizes,  $x = 3, 5-10$ , Mn<sub>*x*</sub>As clusters show ferrimagnetic coupling. It is suggested that, if grown during the low temperature MBE, the giant magnetic moments due to ferromagnetic coupling in Mn<sub>2</sub>As and Mn<sub>4</sub>As clusters could play a role on the ferromagnetism and on the variation observed in the Curie temperature of Mn-doped III-V semiconductors.

PACS numbers: 61.46.+w, 36.40.Cg, 75.50.Pp

Manganese is a unique *3d* transition metal element due to its unusual and fascinating electronic and magnetic behavior as atom, cluster, crystal and as well as impurity. The filled *4s* and half-filled *3d* shell and the large energy gap  $\sim 8$  eV between them prevent significant *s* – *d* hybridization and therefore they do not bind strongly as Mn atoms begin to form cluster[1, 2]. Similarly,  $\alpha$ -Mn, the most stable form of bulk Mn, has the least binding energy among all the *3d* transition metal elements. The magnetic properties of Mn clusters are particularly interesting. An early electron spin resonance study on small Mn clusters in an inert matrix suggested ferromagnetic ordering with magnetic moment  $5 \mu_B$ /atom [3]. More recently, through Stern-Gerlach (SG) molecular beam experiment [4], Knickelbein found that manganese clusters in the size range Mn<sub>5</sub> - Mn<sub>99</sub> display ferrimagnetic ordering with a maximum magnetic moment  $\sim 1.72 \mu_B$ /atom for Mn<sub>12</sub>, despite of the fact that no known bulk phase of Mn displays such ordering. Recent density functional theory (DFT) calculations [1, 2] confirm this ferrimagnetic coupling in the size range  $x \geq 5$  in Mn<sub>*x*</sub> clusters.

Manganese doped semiconductors, such as (GaMn)As and (InMn)As have attracted considerable attention because of their carrier induced ferromagnetism [5]. The Mn dopants in these III-V dilute magnetic semiconductors serve the dual roles of provision of magnetic moments and acceptor production. Earlier experimental results on Ga<sub>1-*x*</sub>Mn<sub>*x*</sub>As indicate a nonmonotonic behavior of Curie temperature  $T_c(x)$ , first increases with the Mn concentration *x*, reaching a maximum of 110 K for  $x \sim 5\%$  and then decreases with the further increase of *x*. However, recent experimental studies [6, 7], under carefully controlled growth and annealing conditions, suggest that the *metastable* nature and high *defect* content of low temperature molecular beam epitaxy (MBE) grown Ga<sub>1-*x*</sub>Mn<sub>*x*</sub>As may be playing an important role in determining the magnetic properties. In particular, under suitable conditions, careful annealing could lead to an

enhancement in  $T_c$  with increasing Mn content [6, 7]. Chiba *et al.* [6] have reported a maximum  $T_c$  as high as 160 K, for 7.4 % Mn concentration, in a layered structure. However, the detailed microscopic nature and the role of the *metastable defects* in Ga<sub>1-*x*</sub>Mn<sub>*x*</sub>As are not yet well understood both theoretically and experimentally and demands more investigation. Strong segregation tendency of the doped transition metal atoms into the semiconductor host [8] makes Mn clustering, around As in Ga<sub>1-*x*</sub>Mn<sub>*x*</sub>As samples, a very important issue.

In this Letter, we address the possibility of such clustering of Mn around As, and if so, then what is the nature of Mn-Mn magnetic coupling? We have, indeed, found that the binding energy of Mn clusters are substantially enhanced by single As doping by having their hybridized *s* – *d* electrons bond with *p* electrons of As. This *stabilization* is accompanied by the *ferromagnetic* or *ferrimagnetic* coupling between Mn atoms, all of which results in the large cluster magnetic moments, which could play a crucial role in the observed ferromagnetism and determining the Curie temperature  $T_c$ , in Mn-doped GaAs and InAs.

Calculations have been carried out using DFT, within the plane wave method [9]. We have employed projector augmented-wave method [10] and Perdew-Burke-Ernzerhof exchange-correlation functional [11] for the spin-polarized generalized gradient approximation (GGA), as implemented in the VASP package [12]. The wave functions are expanded in a plane wave basis set with the kinetic energy cutoff equal to 337.3 eV and the calculations were carried out at the  $\Gamma$  point. The *3d*, *4s* for Mn and *4s*, *4p* orbitals for As were treated as valence states. Symmetry unrestricted geometry optimizations were performed using quasi Newtonian and conjugate gradient methods until all the force components are less than  $0.005$  eV/Å. Simple cubic supercells are used with neighboring clusters separated by at least  $12\text{\AA}$  vacuum regions. Several initial structures were studied

to ensure that the globally optimized geometry does not correspond to the local minima, as well as, for all clusters, we have explicitly considered *all possible* spin multiplicities to determine the ground state magnetic moment.

We begin our discussions with pure  $Mn_x$  ( $x \leq 10$ ) clusters, some of which ( $x \leq 7$ ) have also been studied previously within the all-electron calculation and different levels of GGA [2]. We have found ferromagnetic coupling for  $Mn_2$ ,  $Mn_3$  and  $Mn_4$  with magnetic moment  $5 \mu_B$ /atom, the Hund's rule value for the free atom. Emergence of ferrimagnetic coupling starts from  $Mn_5$ . The total magnetic moments of  $Mn_x$  clusters corresponding to the ground state geometries, for  $x = 5-10$ , are 3, 8, 5, 8, 7 and  $14 \mu_B$  respectively (see Table I), which are in excellent agreement with the recent SG experiment [4]. Because of the half-filled  $3d$  and filled  $4s$  shell and a substantial gap between them, we found  $Mn_2$  is a weakly bound van der Waals (vdW) dimer with bond length  $2.58 \text{ \AA}$  and binding energy  $0.53 \text{ eV/atom}$ , as it is evident from the low experimental value [13]. Antiferromagnetic  $Mn_2$  dimer is  $0.53 \text{ eV}$  higher in energy, whereas for  $Mn_3$ , the frustrated antiferromagnetic structure is almost degenerate ( $0.05 \text{ eV}$  higher in energy) with the ferromagnetic structure. As  $x$  increases, binding energy increases monotonically [Fig.1(a)], reaches a value  $1.94 \text{ eV/atom}$ , 66% of bulk  $\alpha$ -Mn, for  $Mn_{10}$ . We note, generally, the Mn-Mn bonds between like spins are larger ( $2.30-2.85 \text{ \AA}$ ) than that of between opposite spins ( $2.20-2.75 \text{ \AA}$ ). Several isomers lying close in energy to the ground state of  $Mn_x$  were found which will be discussed elsewhere [1], in detail.

In the Fig.??, we depict the ground state geometries of  $Mn_xAs$  clusters with their spin ordering. The MnAs dimer has much higher binding energy,  $1.12 \text{ eV/atom}$ , and much shorter bond length,  $2.21 \text{ \AA}$ , than the  $Mn_2$  vdW dimer. We have repeated the calculations of MnAs dimer, including Mn  $3p$  as valence state [14], and have obtained an optimized bond length  $2.22 \text{ \AA}$  and binding energy  $1.08 \text{ eV/atom}$  with same total magnetic moment.

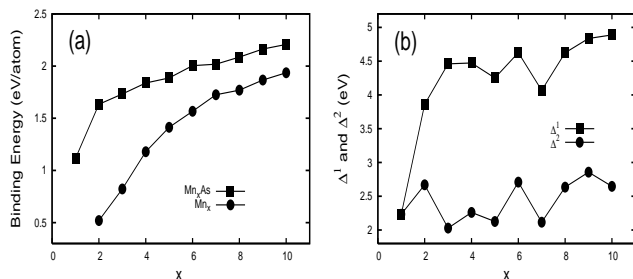


FIG. 1: (a) Plot of binding energy/atom with  $x$ , for  $Mn_x$  and  $Mn_xAs$ . (b) Two energy gains,  $\Delta^1$  and  $\Delta^2$ , are plotted with  $x$ . These energy gains are defined as,  $\Delta^1 = - [E(Mn_xAs) - E(Mn_x) - E(As)]$  and  $\Delta^2 = - [E(Mn_xAs) - E(Mn_{1-x}As) - E(Mn)]$ .

Binding energy increases substantially to  $1.63 \text{ eV/atom}$  for the isosceles triangular  $Mn_2As$ . The Mn-Mn distance,  $2.59 \text{ \AA}$ , in  $Mn_2As$  is almost equal to the Mn-Mn distance in  $Mn_2$ ,  $2.58 \text{ \AA}$ , and Mn-As-Mn bond angle is found to be  $68^\circ$ . As more Mn atoms are added, the structures take three-dimensional shape, and the determination of ground state become a delicate task, as more than one geometric and/or magnetic isomers, very close in energy to the ground state are found, which will be presented elsewhere in detail. As mentioned earlier, this was done by minimizing the total energy of each cluster with respect to *all possible* spin multiplicities for every geometric structure studied. The presence of an As atom makes  $Mn_3As$  cluster tetrahedral, however,  $Mn_4As$  is a  $Mn_4$  tetrahedron with As at a face cap.  $Mn_6As$  is the only cluster whose geometry differs significantly from a pure  $Mn_6$  cluster.  $Mn_6$  is octahedral, whereas  $Mn_6As$  is a pentagonal bipyramid, where the As atom is trapped in the pentagonal ring. As  $x$  in  $Mn_xAs$  increases, binding energy increases very slowly from  $1.63 \text{ eV/atom}$  for  $Mn_2As$  and tends to saturate to a value  $2.21 \text{ eV/atom}$  for  $Mn_{10}As$  (Fig.1(a)). The *shortest* Mn-As bond length increases from  $2.21 \text{ \AA}$  for MnAs to  $2.46 \text{ \AA}$  for  $Mn_{10}As$ , which is 4% and 2% shorter than the Mn-As distance in  $\alpha$ -MnAs and  $Ga_{1-x}Mn_xAs$ , respectively, whereas the *shortest* Mn-Mn distance decreases from  $2.59 \text{ \AA}$  for  $Mn_2As$  to  $2.23 \text{ \AA}$  for  $Mn_{10}As$ . Generally, we find the same trend as seen in the pure  $Mn_x$  clusters that the bonds between Mn atoms of opposite spin to be somewhat shorter ( $2.20-2.60 \text{ \AA}$ ) than the bonds between Mn atoms of like spin ( $2.50-2.90 \text{ \AA}$ ), whereas all Mn-As distances vary between  $2.20-2.60 \text{ \AA}$ . All the Mn-As-Mn bond angles in these clusters vary in between  $\sim 60-70^\circ$ . All the clusters in the Fig.?? and their respective isomers are magnetically stable i.e. both the spin gaps are positive: the lowest unoccupied molecular orbital of the minority (majority) spin lies above the highest occupied molecular orbital of the majority (minority) spin. These two spin gaps,  $\delta_1$  and  $\delta_2$  [15], for  $Mn_2As$  ( $0.83$  and  $1.34 \text{ eV}$ ) and  $Mn_4As$  ( $0.89$  and  $1.14 \text{ eV}$ ) are the highest among all clusters. As  $x$  increases,  $\delta_1$  and  $\delta_2$  decrease to a value  $0.47$  and  $0.35 \text{ eV}$ , respectively, for  $Mn_{10}As$ .

The next important issue is to see whether these Mn clustering around single As are at all energetically favorable or not. To understand this point, we calculate two different energy gains,  $\Delta^1$  - the energy gain in adding an As atom to a  $Mn_x$  cluster and  $\Delta^2$  - the energy gain in adding a Mn atom to a  $Mn_{1-x}As$  cluster. Fig.1(a) shows that due to the lack of hybridization between the  $4s$  and the  $3d$  electrons binding energy of pure  $Mn_x$  clusters are very small. However, as an As atom is attached, the  $4s^2$  electrons of Mn interact with the  $4p^3$  electrons of As, which results in the substantial enhancement in the bonding (Fig.1(a)), and consequently,  $\Delta^1$  increases with  $x$ , which finally tends to saturate (Fig.1(b)).  $\Delta^2$  gives the number that how many Mn atoms can be bonded to

TABLE I: Total cluster magnetic moments  $\mu_x$  of pure  $\text{Mn}_x$  and  $\text{Mn}_x\text{As}$  clusters, corresponding to the ground state, for cluster size  $x \leq 10$ .

$x$	$\mu_x(\mu_B)$		$x$	$\mu_x(\mu_B)$	
	$\text{Mn}_x$	$\text{Mn}_x\text{As}$		$\text{Mn}_x$	$\text{Mn}_x\text{As}$
1	5	4	6	8	9
2	10	9	7	5	6
3	15	4	8	8	7
4	20	17	9	7	10
5	3	2	10	14	13

a single As atom, which is still significant, 2.65 eV, for  $\text{Mn}_{10}\text{As}$ . These behaviors of  $\Delta^1$  and  $\Delta^2$  indicate that the Mn clusters around As are energetically favorable and we, therefore, argue that they are, likely to be, present in the low temperature MBE grown (GaMn)As/(InMn)As.

Now we ask the next and most important question that what is the Mn-Mn magnetic coupling in these  $\text{Mn}_x\text{As}$  clusters? The total magnetic moments of  $\text{Mn}_x\text{As}$  clusters corresponding to the ground state geometries are given in Table I. These large magnetic moments generally arise from the ferrimagnetic coupling between the moments at Mn sites with the exceptions for  $\text{Mn}_2\text{As}$  and  $\text{Mn}_4\text{As}$ , where the magnetic coupling is ferromagnetic. We note, generally, no change in the nature of magnetic coupling between the Mn sites in  $\text{Mn}_x\text{As}$  clusters from their respective pure  $\text{Mn}_x$ . However, only for  $\text{Mn}_3\text{As}$ , the Mn-Mn coupling behavior changes from ferromagnetic to ferrimagnetic, due to As doping, where a ferromagnetic tetrahedral structure with total moment  $12 \mu_B$  is found to be 0.12 eV higher. The nature of the magnetic coupling is clear from their respective constant spin density surfaces, which are plotted for  $\text{Mn}_2\text{As}$ ,  $\text{Mn}_3\text{As}$ ,  $\text{Mn}_4\text{As}$  and  $\text{Mn}_8\text{As}$  in the Fig.???. The ground state magnetic moments of  $\text{Mn}_x\text{As}$ , for  $x=1, 2, 3, 5, 7, 8$  and  $10$  can be represented as  $(\mu_x - 1) \mu_B$ , whereas for  $x=4$  and  $9$ , it can be expressed as  $(\mu_x - 3) \mu_B$ , where  $\mu_x$  is the total magnetic moment of the  $\text{Mn}_x$  cluster corresponding to the ground state or the first isomer [1]. Local magnetic moment,  $M$ , at each site can be calculated by  $M = \int_0^R [\rho_\uparrow(\mathbf{r}) - \rho_\downarrow(\mathbf{r})] d\mathbf{r}$ , where  $\rho_\uparrow(\mathbf{r})$  and  $\rho_\downarrow(\mathbf{r})$  are up-spin and down-spin charge densities, respectively, and  $R$  [16] is the radius of a sphere centring the atom. For MnAs dimer, the magnetic moment at Mn site,  $M_{Mn}$ , and at As site,  $M_{As}$ , are  $3.72 \mu_B$  and  $-0.26 \mu_B$ , respectively. This large negative polarization of the anion, As, is due to the strong  $p-d$  interaction. In the  $\text{Mn}_2\text{As}$  cluster, Mn atoms are ferromagnetically coupled with  $M_{Mn}=3.79 \mu_B$  each, whereas  $M_{As}$  is  $-0.14 \mu_B$ . Mn atoms in the  $\text{Mn}_3\text{As}$  take frustrated antiferromagnetic structure with  $M_{Mn} = 3.1, 3.1$  and  $-3.9 \mu_B$  and  $M_{As}$  has a value  $-0.21 \mu_B$ . For  $\text{Mn}_4\text{As}$ , Mn atoms are ferromagnetically arranged (Fig.???) with an average  $M_{Mn}=3.66 \mu_B$  and are coupled antiferromagnetically with the As atom,  $M_{As}=-0.22 \mu_B$ . For  $\text{Mn}_5\text{As}$ ,  $M_{Mn}$  varies between  $3.04-3.72 \mu_B$  with a

local magnetic moment  $-0.23 \mu_B$  at As site. Polarized neutron diffraction study found a local magnetic moment of  $-0.23 \pm 0.05 \mu_B$  at the As sites for NiAs-type MnAs [17], which is very close to the present values for MnAs -  $\text{Mn}_5\text{As}$  clusters. These Mn-Mn magnetic behavior are unlike the previous study of nitrogen-doped  $\text{Mn}_x$  clusters,  $x=1-5$ , by Rao and Jena [18], where Mn atoms were found to be coupled ferromagnetically for all sizes. We observe, the negative polarization of As,  $M_{As}$ , decreases sharply to  $-0.08 \mu_B$  for  $\text{Mn}_6\text{As}$  and further decreases monotonically to  $-0.02 \mu_B$  for  $\text{Mn}_8\text{As}$ , however it becomes positive, 0.04 and 0.02, for  $\text{Mn}_9\text{As}$  and  $\text{Mn}_{10}\text{As}$ , respectively. For all  $\text{Mn}_x\text{As}$  clusters,  $x=6-10$ , Mn atoms are coupled ferrimagnetically, and  $M_{Mn}$  of highly coordinated atoms are very small than those of the surface atoms and it varies between 0.8 -  $3.7 \mu_B$ .

In conclusion, though the As atom induces clustering of Mn, the individual magnetic moments of Mn couple ferromagnetically only for  $\text{Mn}_2\text{As}$  and  $\text{Mn}_4\text{As}$  clusters and, however, ferrimagnetically aligned for all other sizes. Not only that, the ferromagnetic  $\text{Mn}_2\text{As}$  and  $\text{Mn}_4\text{As}$  are even more stable than other sized ferrimagnetic clusters, as they have largest spin gaps. We believe that Mn clustering, during the low temperature MBE growth, could be responsible for the ferromagnetism and reported high  $T_c$  in (GaMn)As and should be taken into account to formulate an adequate theory of ferromagnetism in III-V semiconductors [19]. If Mn-doped GaAs, under carefully controlled growth and annealing condition, contains  $\text{Mn}_2\text{As}$  and/or  $\text{Mn}_4\text{As}$  clusters, which have large cluster magnetic moments, would enhance the local magnetic moment and consequently could enhance  $T_c$ . On the other hand, large clustering would yield low  $T_c$  due to their small local magnetic moment. This study also suggest that the similar mechanism could enhance the  $T_c$  of (InMn)As and further investigation of Mn-clustering around oxygen could explain the ferromagnetism and observed high  $T_c$  of Mn-doped ZnO in the *metastable* phase [20]. EXAFS studies would be very useful to see whether these clusters of Mn around As are, indeed, present in these samples and the gas phase experiments involving Mn clustering in a As-seeded chamber can yield direct information on the magnetic behavior of  $\text{Mn}_x\text{As}$  clusters. We hope, our study will encourage such experiments.

M. K. thankfully acknowledges the congenial hospitality at the Centre for Modelling and Simulation of Pune University. This work has been done under the DST contract SR/S2/CMP-25/2003.

\* Corresponding author

- [1] M. Kabir, D. G. Kanhere and A. Mookerjee, (To be Published.)
- [2] P. Bobadova-Parvanova, K. A. Jackson, S. Srinivas and M. Horoi, Phys Rev. A. **67**, 61202(R) (2003); J. Chem.

- Phys. **122**, 14310 (2005); N. O. Jones, S. N. Khanna, T. Baruah and M. R. Pederson, Phys. Rev. B **70**, 45416 (2004).
- [3] R. J. Van Zee and W. Weltner, Jr., J. Chem. Phys. **89**, 4444 (1988); C. A. Bauman, R. J. Van Zee, S. Bhat, and W. Weltner, Jr., J. Chem. Phys. **78**, 190 (1983).
- [4] M. B. Knickelbein, Phys. Rev. Lett. **86**, 5255 (2001); Phys. Rev. B **70**, 14424 (2004)
- [5] H. Ohno *et al.*, Appl. Phys. Lett. **69**, 363 (1996), H. Ohno, J. Magn. Mater **200**, 110 (1999); Science **281**, 951 (1998).
- [6] D. Chiba, K. Tankamura, F. Matsukura and H. Ohno, Appl. Phys. Lett **82**, 3020 (2003)
- [7] K. W. Edmonds *et al.*, Appl. Phys. Lett **81**, 4991 (2002); S. J. Potashnik *et al.*, *ibid* **79** 1495 (2002); K. C. Ku *et al.*, *ibid* **82**, 2302 (2003)
- [8] M. Zajac *et al.*, J. Appl. Phys. **93**, 4715 (2003); S. R. Shinde *et al.*, Phys. Rev. B **67**, 115211 (2003).
- [9] J. Ihm, A. Zunger and M.L. Cohen, J. Phys. C **12**, 4409 (1979).
- [10] G. Kresse and J. Joubert, Phys. Rev. B **59**, 1758 (1999).
- [11] J. P. Perdew, K. Burke, and M. Ernzerhof, Phys. Rev. Lett. **77**, 3865 (1996).
- [12] G. Kresse and J. Furthmuller, Phys. Rev. B. **54**, 11169 (1996).
- [13] M. D. Morse, Chem. Rev. **86**, 1049 (1986).
- [14] For MnAs dimer, inclusion of Mn  $3p$  as valence states systematically underestimates total energy by an amount  $\sim 0.04$  eV/atom, for all possible total moment, 0-8  $\mu_B$ , and overestimates the corresponding bondlength by a maximum of 0.01 Å.
- [15]  $\delta_1 = -(\epsilon_{HOMO}^{majority} - \epsilon_{LUMO}^{minority})$  and  $\delta_2 = -(\epsilon_{HOMO}^{minority} - \epsilon_{LUMO}^{majority})$ .
- [16] This procedure captures at least 85% of the total moment for the clusters.  $R_{Mn}$  is taken 1.10 Å for all  $x$ , whereas,  $R_{As}$  are 1.11, 1.22 and 1.30 Å for  $x=1,2$  and 3-10, respectively.
- [17] Y. Yamaguchi and H. Watanabe, J. Magn. Mater. **31-34**, 619 (1983).
- [18] B. K. Rao and P. Jena, Phys. Rev. Lett. **89**, 185504 (2002).
- [19] P. Mahadevan and A. Zunger, Phys. Rev. B **68**, 75202 (2003); M. v. Schilfgaarde and O. N. Mryasov, Phys. Rev. B **63**, 233205 (2001).
- [20] C. Darshan *et al.*, Nature Materials **3**, 709 (2004).

### Figure Captions

1. Ground state geometries and the corresponding spin ordering of  $Mn_xAs$  clusters,  $x=1-10$ . Blue and red balls represent  $Mn_{\uparrow}$  and  $Mn_{\downarrow}$  atoms, respectively. Green ball represents the As atom. The bond lengths are given in Å. Magnetic polarization of As, is negative for  $MnAs - Mn_8As$  and, whereas, positive for  $Mn_9As$  and  $Mn_{10}As$ . Note, Mn-Mn interaction is ferromagnetic only for  $Mn_2As$  and  $Mn_4As$  clusters and ferrimagnetic for all other sizes.

2. (a) Plot of binding energy/atom with  $x$ , for  $Mn_x$  and  $Mn_xAs$ . (b) Two energy gains,  $\Delta^1$  and  $\Delta^2$ , are plotted with  $x$ . These energy gains are defined as,  $\Delta^1 = -[E(Mn_xAs) - E(Mn_x) - E(As)]$  and  $\Delta^2 = -[E(Mn_xAs) - E(Mn_{1-x}As) - E(Mn)]$ .

3. Constant spin density surfaces for  $Mn_2As$ ,  $Mn_3As$ ,  $Mn_4As$  and  $Mn_8As$  corresponding to 0.04, 0.04, 0.04 and 0.02  $e/\text{Å}^3$ , respectively. Red and blue surfaces represent positive and negative spin densities, respectively. Green ball is the As atom, which has negative polarization in all these structures. Note ferromagnetic ( $Mn_2As$  and  $Mn_4As$  (left panel)) and ferrimagnetic ( $Mn_3As$  and  $Mn_8As$  (right panel)) coupling between Mn atoms.

This figure "kabir\_structure\_Fig1.jpg" is available in "jpg" format from:

<http://arxiv.org/ps/physics/0503009v1>

This figure "kabir\_spindensity\_Fig3.jpg" is available in "jpg" format from:

<http://arxiv.org/ps/physics/0503009v1>